BMC Genomics

RESEARCH

Open Access

Function of floral fragrance-related microRNAs and their targets in *Hedychium coronarium*

Fang Wang[1†], Liang Liu[1†], Rangcai Yu[2], Xin Li[1], Yunyi Yu[1], Xinyue Li[1], Yuechong Yue[1] and Yanping Fan[1*]

Abstract

Background *Hedychium coronarium* is highly valued for its intense fragrance, which may be influenced by the expression of microRNAs (miRNAs). miRNAs are a class of small RNAs that play conserved and pivotal regulatory roles throughout plant growth and development, modulating various aspects of plant metabolism. However, the specific roles of miRNAs in the growth and development of *H. coronarium* remain largely uncharacterized.

Results To identify miRNAs in *H. coronarium* and assess their potential role in the synthesis of floral fragrance compounds, we analyzed the volatile compounds and miRNA expression patterns at three developmental stages (F1, F5, F6). Our findings revealed that the volatile emissions of major floral compounds, including eucalyptol, ocimene, and linalool, increased as the flowers progressed through development. Small RNA sequencing identified 171 conserved miRNAs from 24 miRNA families, along with 32 novel miRNAs. Degradome sequencing uncovered 102 mRNA degradation sites corresponding to 90 target genes from 30 miRNA families. Quantitative RT-PCR (qRT-PCR) analysis showed that the expression of hco-miR393a and hco-miR167n mirrored the release pattern of floral fragrance compounds, while the expression of *HcTIR1* and *HcARF8* inversely correlated with those of hco-miR393a and hco-miR167n. Co-transformation experiments in tobacco confirmed that *HcTIR1* and *HcARF8* are direct targets of hco-miR393a and hco-miR167n, respectively. Additionally, treatments with exogenous IAA and the auxin inhibitor PCIB modulated both the release of floral volatiles and the expression of hco-miR393a and hco-miR167n. STTM and VIGS experiments further indicated that hco-miR167n and hco-miR393a positively regulate floral fragrance metabolism, while *HcARF8* and *HcTIR1* act as negative regulators. Finally, dual-luciferase and yeast one-hybrid assays demonstrated that *HcARF8* binds to the promoter of the terpene synthase gene *HcTPS8*, thereby regulating the biosynthesis of floral fragrance compounds.

Conclusions This study represents the first comprehensive identification of miRNAs in *H. coronarium* and the characterization of their expression profiles in petal tissues at various developmental stages. These findings offer novel insights into the molecular mechanisms governing the synthesis of floral fragrance compounds and highlight the critical role of miRNAs in the regulation of metabolic processes within the Zingiberaceae family.

Keywords *H. coronarium*, miRNAs, Floral fragrance compounds, Degradome sequencing

†Fang Wang and Liang Liu contributed equally to this work.

*Correspondence:
Yanping Fan
fanyanping@scau.edu.cn
[1]The Research Center for Ornamental Plants, College of Horticulture, South China Agricultural University, Guangzhou 510642, China
[2]College of Life Sciences, South China Agricultural University, Guangzhou 510642, China

Background

The study of gene expression and its regulatory mechanisms is crucial for understanding plant growth and development. Small RNAs (sRNAs) play significant roles in regulating plant metabolism, hormone responses, and responses to various stresses [1]. Among them, microRNA (miRNAs) play important regulatory roles post-transcriptionally in eukaryotic organisms [2]. miRNAs are a class of conserved endogenous sRNAs in plants and animals, typically 18–25 nucleotides in length. They regulate the expression of target genes/mRNAs post-transcriptionally in a sequence-specific manner, usually negatively affecting mRNA accumulation [3]. Extensive research has demonstrated that miRNAs play roles in plant growth, development, hormone signaling, and responses to environmental stresses. For instance, in rice, OsmiR396d targets the *OsGRF6* gene, participating in gibberellin biosynthesis and signaling, thereby controlling plant height [4]. In Papaya, cpa-miR390a targets *CpARF19*, participating in ethylene and auxin signaling pathways, thus influencing papaya ripening [5]. In *Arabidopsis thaliana*, miR160 regulates hypocotyl elongation by downregulating ARF genes [6], while miR319 promotes cell proliferation by negatively regulating TCP4 [7]. However, miRNAs in *Hedychium coronarium* remain poorly understood to date. Therefore, it is essential to investigate miRNAs and their targets in *H. coronarium*.

Furthermore, extensive research indicates that miRNAs play a crucial role in regulating the expression of genes related to flower development in plants. For example, miR397 modulates flowering time through the targeted regulation of the LAC15 gene [8]. MiR156 and miR157 prevent early flowering by inhibiting the translation of the SPL3 gene [9]. MiR159 alters flower color and the formation of floral meristems by targeting MYB transcription factors in the GA pathway [10]. miR172 controls the size of floral meristems by regulating the expression of AP2 genes [11]. miR164 regulates the number of petals by targeting the CUC1 and CUC2 genes, which encode NAC domain proteins [12]. Studies on miRNAs in horticultural plants have primarily focused on the regulation of floral organ development, but there is limited information on miRNAs in aromatic plants, which restricts the breeding of fragrant plants.

Currently, with the development of high-throughput sequencing technology, a new method for detecting miRNA targets, known as degradome sequencing, has emerged. This technique combines the advantages of high-throughput deep sequencing and bioinformatics analysis. In this method, deep sequencing analysis is performed on the degraded fragments of target mRNAs cleaved by miRNAs to identify miRNA targets [13]. This approach has already been successfully applied to the study of miRNA targets in *Arabidopsis* [14], rice [15], and maize [16]. Kim et al. [17] conducted sRNA sequencing on *Rosa* and identified 267 miRNAs, including 25 novel miRNAs and 242 conserved miRNAs, which play important roles in the flower development and phenotypes of roses. Jin et al. [18] performed sRNA sequencing on peony (*Paeonia ostii*) flower buds, discovering 12 conserved miRNAs and 18 novel miRNAs that are involved in the response to copper stress.

The regulation of hormone homeostasis mediated by miRNAs is a highly conserved process, with interactions between miRNAs and plant hormones, especially auxins, forming critical regulatory nodes in plant development. As a core plant hormone, auxin coordinates various physiological processes through dynamic distribution and signal transduction, while miRNAs finely tune these pathways via post-transcriptional regulation of auxin-related genes [19]. For example, the miR160-ARF10/16/17 and miR167-ARF6/8 modules not only regulate auxin homeostasis but also integrate environmental signals with developmental programs [20, 21]. miR393 targets auxin receptors Transport Inhibitor Response 1 (TIR1) and auxin signaling F-box proteins (AFB), thereby modulating growth, development, and stress response processes in various plants [22]. Studies have shown that this miRNA-auxin co-regulation affects floral organ morphogenesis, aromatic metabolite accumulation, and stress adaptability in model plants. However, whether this conserved regulatory pattern exists in the auxin-mediated biosynthesis of aromatic compounds in *H. coronarium* remains to be systematically investigated and confirmed.

H. coronarium is a perennial herbaceous plant belonging to the Zingiberaceae family. It is known for its beautiful flower shape and strong fragrance, making it widely used in horticultural breeding and the fresh-cut flower market, with significant economic and ecological value. Currently, research on the regulatory mechanisms of *H. coronarium* flower fragrance is substantial, with particular emphasis on terpene synthase studies. Specifically, both *HcTPS5* and *HcTPS8* catalyze the production of linalool from GPP, whereas *HcTPS7* predominantly converts GPP into sabinene [23, 24]. However, the regulatory mechanisms of miRNAs in the growth, development, and synthesis of fragrance compounds in *H. coronarium* remain unclear. This lack of understanding significantly limits the progress of breeding improvement. Therefore, the identification and analysis of miRNAs, prediction of their target genes, and elucidation of their mechanisms of action will become new directions in *H. coronarium* research. This study is the first to use high-throughput sRNA sequencing technology to identify miRNAs at different developmental stages of *H. coronarium*. Combining GC-MS, degradome sequencing, and bioinformatics analysis, we predicted the target genes of miRNAs and

identified miRNAs related to fragrance. Molecular biology techniques were used to validate the functions of these miRNA target genes and the molecular mechanisms regulating fragrance, providing a theoretical basis for transcriptional regulation in the synthesis of aromatic compounds in *H. coronarium*.

Materials and methods

Plant material

Hedychium coronarium was cultivated under natural light conditions in the horticultural greenhouse at South China Agricultural University, Guangzhou, China (23.16°N, 113.36°E) [25]. *H. coronarium* is a perennial herbaceous plant belonging to the Zingiberaceae family. The plant is grown in the controlled greenhouse under conditions: 26 ± 2℃ and 75–80% humidity. Yanping Fan undertook the formal identification of the plant material used in the study, and no voucher specimens were collected. Based on the flowering stage of *H. coronarium*, six stages (F1 ~ F6) were identified (Fig. 1). Petals from the budding stage (F1), full blooming stage (F5), and senescence stage (F6) were collected as experimental materials, then frozen in liquid nitrogen, and stored in refrigerator at -80 ℃.

Identification of volatile aroma compounds in *H. coronarium*

Three flowers from the same developmental stage of *H. coronarium* were weighed and placed into a clean glass bottle. A total of 2 μL of ethyl caprate was added as an internal standard, and the bottle was sealed and allowed to react for 15 min. Subsequently, a high-temperature activated extraction needle (SPEM, 50/30 μm, DVB/CAR/PDMS) from the GC-MS instrument was inserted into the glass bottle for headspace extraction over a period of 15 min. The extraction needle was then transferred to the GC-MS inlet for injection, and removed once the injection was completed. All samples were analyzed using an Agilent 7890 A gas chromatograph coupled with a 5975 C mass spectrometer.

The chromatographic separation was carried out using an Agilent DB-5MS capillary column (122–5532; 30 m, I.D. 0.25 mm, film thickness 0.25 μm). The operating conditions were set as follows: the injection port temperature was 250 °C with no split, the column head pressure was 50 Pa, and the flow rate was 1 mL/min. The sampling time ranged from 3 to 5 min. The oven temperature was initially held at 40 °C for 2 min, then increased from 40 °C to 250 °C at a rate of 10 °C/min, followed by a 5-minute hold at 250 °C. The ion source temperature of the mass spectrometer was maintained at 230 °C, while the interface temperature was set at 280 °C. Electron impact ionization was applied with a mass range of 50–550 amu. Gas chromatography effectively separated volatile components, with individual compounds forming distinct chromatographic peaks. The mass spectrometer was used for the qualitative identification of these components, and their mass spectra were analyzed using the NIST 2008 library to determine the chemical composition of volatile substances in different samples. Quantification was performed using a relative quantification method.

Fig. 1 Photographs of *H. coronarium* petals at different developmental stages

RNA extraction and sequencing of small RNA

We collected petals of *H. coronarium* at the F1 (the budding stage), F5(the full blooming stage), and F6 stages (the senescence stage) for RNA extraction. And RNA was extracted using the HiPure Plant RNA Mini Kit (Magen, Guangzhou, China) according to the manufacturer's protocol, with three biological replicates for each treatment. The RNA samples were then assessed for purity, concentration, and integrity using a Nanodrop spectrophotometer to ensure the quality of the samples for sequencing. Samples meeting the purity standards were sent to Novogene Company (Beijing, China) for library construction and Illumina sequencing. Small RNA libraries for the F1, F5, and F6 stages were constructed. After the removal of low-quality reads, clean reads were aligned and annotated against the Silva, GtRNAdb, Rfam, and Repbase databases using Bowtie software. Non-coding RNAs, including ribosomal RNA, transfer RNA, nuclear small RNA, and repetitive sequences, were removed, resulting in unannotated reads.

Prediction of miRNA target genes

Three qualitative degradome libraries were constructed to identify miRNA target transcripts. The filtered unannotated reads were aligned with miRNAs from all species in the miRBase 22.1 database to identify known miRNAs in *H. coronarium*. MiRDeep2 and Mfold software were employed to predict the secondary structures of unannotated miRNAs and their precursor sequences, enabling the discovery of novel miRNAs. Target genes for both known and novel miRNAs were predicted using psRNA-Target. BLAST software was then used to align the predicted target gene sequences with the GO, KEGG, and Rfam databases to obtain functional annotation information for the target genes.

RT-qPCR expression analysis of target genes

The forward and reverse primers for miRNA target genes were designed using Premier 5.0 software. Quantitative PCR was performed on the ABI7500 fluorescence quantitative PCR system with a reaction volume of 20 μL. The reaction mixture included 2 μL of cDNA template, 10 μL of Hieff® qPCR SYBR Green Master Mix (Yeasen Biotechnology, Shanghai, China), 7.2 μL of RNase-free H_2O, and 0.4 μL of each forward and reverse primer. The RPS gene was used as an internal control to normalize the expression levels of target genes. The qRT-PCR program consisted of an initial denaturation at 95℃ for 30 s, followed by 40 cycles of denaturation at 95℃ for 5 s, annealing at 55℃ for 30 s, and extension at 72℃ for 30 s. A melting curve analysis was performed starting at 60℃ and increasing to 95℃ at a rate of 1%. Relative expression levels between treatments were calculated using the $2^{-\triangle\triangle Ct}$ method.

Transient expression analysis

The interaction between miRNAs and their target genes was confirmed in vivo using a transient expression system. Overexpression vectors PMS4-*ARF8/TIR1* and pOx-hco-miR167n/miR393a were constructed. Co-expression of the miRNAs and their target genes was achieved in *Nicotiana benthamiana* leaves via infiltration with *Agrobacterium tumefaciens* strain EHA105. After 3 days of infiltration, GFP fluorescence in the leaves was observed using a laser scanning confocal microscope (Zeiss LSM800).

Effects of exogenous IAA and auxin inhibitor PCIB on fragrance compounds and related genes

Several flower branches at the budding stage were selected and placed individually in conical flasks containing either sterile water (blank control), 0.1 mM IAA, or 350 mg/L PCIB. The flasks were then placed in an artificial growth chamber with a 12-hour photoperiod for cultivation. After the treatment period, petals were harvested for the analysis of volatile fragrance compounds using GC-MS, and the expression of relevant genes was measured by qRT-PCR.

The interaction between miRNA and target gene

To validate the interaction between miRNAs and their target genes, we performed short tandem target mimic (STTM) and barley stripe mosaic virus-mediated (BSMV) virus-induced gene silencing (VIGS) experiments. Specifically, pOx-STTM-miR167n/miR393a vectors and VIGS-*ARF8/TIR1* constructs were generated and transformed into *A. tumefaciens* strain EHA105. The transformed *A. tumefaciens* was subsequently used to infiltrate *H. coronarium*. After a 24-hour incubation, the volatile fragrance compound content was quantified, and the expression levels of aroma-related genes were analyzed.

Dual-luciferase assay

The full-length coding sequence of *HcARF8* was amplified and cloned into the pGreen II 0029 62-SK vector, while the promoters of *HcTPS3*, *HcTPS5*, and *HcTPS8* were inserted into the pGreen II 0800-LUC vector. The primers used for vector construction are listed in Supplemental Table S1. All constructs were verified by sequencing and introduced into *A. tumefaciens* strain GV3101 via heat shock. A dual-luciferase assay was performed in *N. benthamiana* leaves following a standard protocol. Four days post-infiltration, the Dual-Luciferase Reporter Gene Assay Kit (RG027, Beyotime) was used to measure the fluorescence values of firefly luciferase (LUC) and renilla luciferase (REN) using the Thermo Scientific Luminoskan Ascent instrument (Gelview 6000Pro II, China). The relative LUC/REN ratio was then calculated to assess promoter activity.

Yeast one-hybrid (Y1H) assay

The Matchmaker Gold Yeast One-Hybrid Library Screening System (Clontech) was employed to investigate the interaction between *HcARF8* and the promoters of *HcTPS3*, *HcTPS5*, and *HcTPS8*. The promoter fragments of *HcTPS3*, *HcTPS5*, and *HcTPS8* were cloned into the pAbAi vector, while the coding sequence (CDS) of *HcARF8* was inserted into the pGADT7 vector. The recombinant pAbAi-*HcTPS3*, pAbAi-*HcTPS5*, and pAbAi-*HcTPS8* constructs were linearized and transformed into the Y1HGold yeast strain to test for promoter autoactivation. Subsequently, the pGADT7-*HcARF8* vector was co-transformed with pAbAi-*HcTPS3*, pAbAi-*HcTPS5*, or pAbAi-*HcTPS8* into Y1HGold. As negative controls, the empty pGADT7 vector was co-transformed with the promoter-pAbAi constructs. The primers used for vector construction are listed in Supplemental Table S1.

Statistical analysis

The data were organized using Microsoft Excel 2019 and analyzed with SPSS software 26.0. Results are presented as the mean ± standard deviation (SD). Statistical significance was assessed using Duncan's multiple range test and Student's t-test.

Results

Changes of volatile compounds in *H. coronarium* during different developmental stages

Volatile aroma compounds were measured in the flowers of *H. coronarium* at the F1, F5, and F6 periods (Fig. 2). Ocimene, linalool, and eucalyptol were identified as the main aroma compounds. The concentrations of these

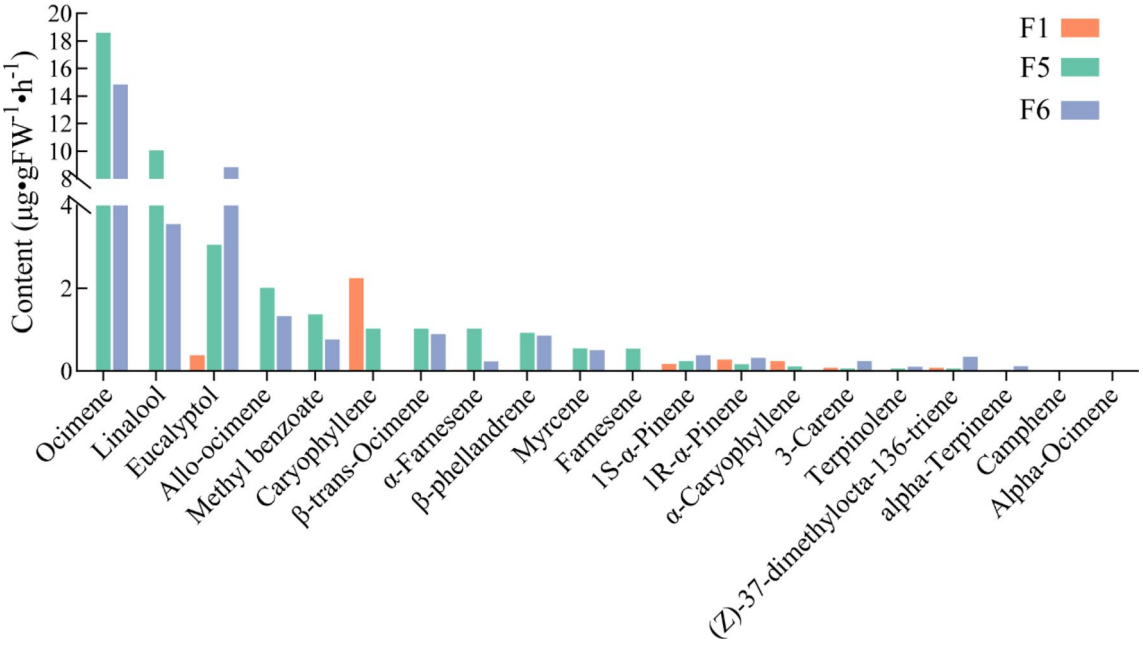

Fig. 2 Changes in volatile aroma compounds during different stages in *H. coronarium*

compounds increased continuously as the flowers developed, reaching the highest levels at the full blooming stage (F5).

Overview of high-throughput small RNA sequencing from *H. coronarium*

Small RNA libraries were constructed from petals of *H. coronarium* at three stages, F1, F5, and F6. For each library, on average, more than 12 million clean reads and over 2.5 million unique reads were obtained (Table S2). The lengths of small RNA sequences from *H. coronarium* were mainly concentrated at 18–30 nt, with the highest number of miRNAs distributed at 23–24 nt in length, which is consistent with the results of miRNA studies of other plant species (Fig. S1).

Screening and analysis of differentially expressed miRNAs in *H. coronarium*

The miRNAs from the three stages of F1, F5, and F6 were compared using DESeq2-EBseq software to screen the differentially expressed miRNAs with conditions set at p-value < 0.05 and$|\log_2(\text{foldchange})| > 1$. As illustrated in Fig. 3, a total of 122 differentially expressed miRNAs were identified across these three stages. Specifically, in the comparison between F5 and F1, 11 miRNAs were upregulated and 7 were downregulated; for F6 versus F1, 51 miRNAs showed upregulation while 42 were downregulated; in the contrast between F6 and F5, 43 miRNAs were upregulated and 35 downregulated. Interestingly, as the flowers developed, the number of up-regulated miRNAs was significantly higher than that of down-regulated miRNAs from F1 to F6. Notably, miR162 was found to be differentially expressed in all three pairwise comparisons (Fig. 3).

Identification of known miRNAs and prediction of novel miRNAs

To identify conserved miRNAs in *H. coronarium*, the unannotated clean reads obtained from sequencing were compared with the conserved miRNAs of known plants in miRbase (version 22.1). A total of 171 known miRNAs were identified in *H. coronarium* belonging to 24 conserved miRNA families (Table S3). Among them, miR396, miR167, miR156, miR166, miR171, miR159, and miR168 contain half of the members. miR396 was the largest family, with 22 members, followed by miR167 and miR156, with 19 and 16 members, respectively (Fig. S2). The composition of bases in miRNA sequences is closely related to their biological properties and secondary structure features. By statistically analyzing the distribution pattern and probability of each base of known miRNAs, it can be seen from Fig. S3 that there is a significant difference in the chances of random assignment of the four bases A, C, G, and U in the sequences of known miRNAs. Across the 22 different positions of the known miRNA sequences, the bases with the greatest probability of occurrence in the stages of F1, F5, and F6 are the bases of U, U, and G, respectively, accounting for 28.98%, 29.87%, and 30.38%. Conversely, the bases with the lowest probability of occurrence in all three stages were C bases, accounting for 20.60%, 16.45%, and 17.72%, respectively. Further analysis of miRNA sequences with varying lengths (Fig. S3) reveals a striking bias towards U as the initial base in samples from F1, F5, and F6 stages,

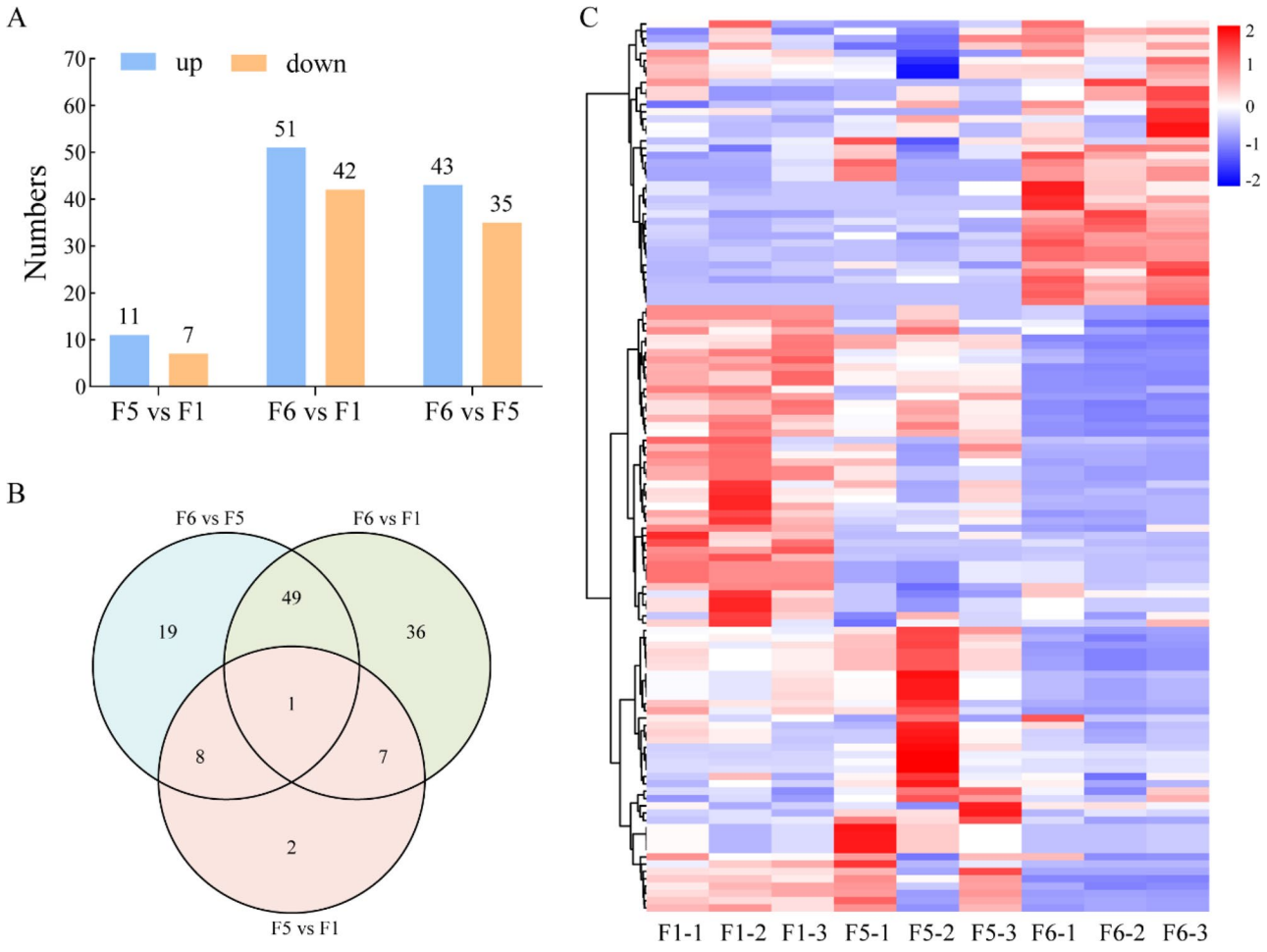

Fig. 3 Expression profile of differentially expressed miRNAs in *H. coronarium*. A, The number of differentially expressed miRNAs; B, Venn diagram of differentially expressed miRNAs; C, Expression profile of differentially expressed miRNAs

with proportions reaching 59.35%, 54.80%, and 49.55%, respectively. This underscores a marked preference for U at both specific sequence locations and as the leading nucleotide in miRNA sequences during these developmental stages.

After identifying known miRNAs, the novel miRNAs were predicted using miREvo and mirdeep2 prediction software, resulting in the identification of 32 novel miRNAs (Table 1). The novel miRNAs are mapped to their respective positions on the *H. coronarium* chromosomes, as shown in Supplementary Fig. S4.

Target prediction of miRNAs using degradome sequencing

To further investigate the regulatory roles of miRNAs, degradome sequencing was performed on petals from three stages: F1, F5, and F6. After discarding low-quality reads and adapter sequences, we obtained 26,333,976 clean reads. Using the TargetFinder target gene prediction software, the miRNAs obtained from high-throughput sequencing of the *H. coronarium* transcriptome database were subjected to target gene prediction (Table S4). For the identification of cleavage sites, the targets were grouped into four categories according to the relative abundance of degradome reads mapping at the predicted miRNA target site relative to the abundance of the reads located at other sites. Representative target plots of identified miRNA targets are shown in (Fig. S5). In Category 0, the peak value of tags was found at the predicted cleavage site of miRNA and there was only one maximum on the transcript. If the abundance of tags was between the median and the maximum, it was grouped as Category 2 or Category 3. In Category 4, the abundance of tags was equal to, or less than the median.

Additionally, a total of 102 miRNA cleavage sites corresponding to 90 target genes across 30 miRNA families were identified, among which 80 target genes were successfully annotated (Table 2), and these targets were predominantly transcription factors. Previous studies have demonstrated that one miRNA can target multiple target genes, and conversely, one target gene can also be targeted by multiple miRNAs. In our study, hco-miR159 had the largest number of predicted target genes, with 10

Table 1 Novel MiRNA sequence information of *H. coronarium*

Novel miRNAs	Sequences	Length	Chr_ID
miRn1	TCAAGCTGTCAGCATGATCTGA	22	000028F_arrow_pilon
miRn2	GGCAAGTCGTTTTTGGCTAGA	21	000040F_arrow_pilon
miRn3	TTTTGGCGTGGTCTCATTAAG	21	000212F_arrow_pilon
miRn4	TCGAGGAAGATGAGTAGGTGG	21	000371F_arrow_pilon
miRn5	CTTCAGATCTGTGCATGTACAC	22	002454F_arrow_pilon
miRn6	TTCCGTATGTGCTTGCAGAAG	21	Hic_asm_0
miRn7	TGGGCTCAAAAGGATAAAGATA	22	Hic_asm_0
miRn8	AACGTATAACTACTGACTTAT	21	Hic_asm_1
miRn9	TCATGTGGGCTCTGACCGCGC	21	Hic_asm_1
miRn10	TTATGGTGCTACTGAATGAGC	21	Hic_asm_1
miRn11	TTGTGGTGCTATTGAATGAGC	21	Hic_asm_1
miRn12	TTGTGGTGCTATTGAATGAGC	21	Hic_asm_1
miRn13	CTTCTGATCTGTGCATGTACAC	22	Hic_asm_10
miRn14	GGCAGATGTAGCCAAGTGGA	20	Hic_asm_11
miRn15	ACTGACTGAGAGCTCTTTCACG	22	Hic_asm_11
miRn16	TTTGATCTTCTGAAGTGCAGG	21	Hic_asm_11
miRn17	ACCGATCGTTTCGAGAAGAGC	21	Hic_asm_11
miRn18	ACCGATCGTTTCGAGAAGAGC	21	Hic_asm_11
miRn19	CGGAGGCGGTGATGGCCGGGGG	22	Hic_asm_11
miRn20	TCATGTCATTCCGATCTCTCT	21	Hic_asm_12
miRn21	CTTTGTGTTGGAGATATTCTTC	22	Hic_asm_13
miRn22	TTTCGTCGCTAAATTTGATGT	21	Hic_asm_14
miRn23	GGCGGGTTGCGAGCTCTTATG	21	Hic_asm_16
miRn24	ATGGCTAGGGACTGGGGGTCT	21	Hic_asm_16
miRn25	CTTCAGATCTGTGCATGTACAC	22	Hic_asm_16
miRn26	TGTGTTGCCTGGGAATTTTGCC	22	Hic_asm_2
miRn27	TATATGGTTGGTGGATCATGA	21	Hic_asm_3
miRn28	TACGTGTTCGTCTAGTTCTCT	21	Hic_asm_4
miRn29	GAGGTCTGTAATTTGATACTGC	22	Hic_asm_5
miRn30	TTTGCATAACTCAGGAGCTGC	21	Hic_asm_9
miRn31	GTGTAGTTTTCCTTTGGCAGG	21	Hic_asm_9
miRn32	TGAGATCATCGATTGCTGGAGA	22	Hic_asm_9

target genes identified, followed by hco-miR396 (8 target genes), and hco-miR156 (7 target genes). Furthermore, through GO and KEGG enrichment analysis of the target genes, it was found that these target genes are predominantly enriched in the plant hormone signal transduction pathway (Fig. S6).

Validation of MiRNA and target gene expression in *H. coronarium*

According to previous studies, the auxin-related signal elements can indirectly regulate the production of volatile compounds in *H. coronarium*. Presently, it is believed that the key signal elements involved in auxin signal transduction are the SCF complex (SKP1-CUL1-TIR1), auxin/ indole-3-acetic acid proteins (Aux/IAAs) and auxin response factor (ARFs) [26]. Combined with the results of miRNA high-throughput sequencing and degradation sequence analysis, it was found that auxin-related signal elements *HcARF8* and *HcTIR1* were paired with hco-miR167n and hco-miR393a, respectively. This suggests that these miRNAs might be involved in the accumulation of volatile fragrance compounds in *H. coronarium* by regulating their respective targets. And the secondary structure predictions for the two miRNAs related to floral fragrance compounds synthesis are shown in Fig. S7.

To preliminarily verify whether hco-miR167n and hco-miR393a are related to the production of volatile compounds in *H. coronarium*, the expression patterns of *HcTIR1*-miR393a and *HcARF8*-miR167n were analyzed by qRT-PCR. The results showed that the expression of hco-miR393a and hco-miR167n was consistent with the release of volatile aroma compounds. Meanwhile, the expression of *HcTIR1* and *HcARF8* was relatively high in the F1 bud stage, remained at a low level throughout the blooming period, and increased slightly in the F6 decline stage (Fig. 4). This suggests that *HcARF8* and *HcTIR1* may be negative regulators of the production of volatile compounds in *H. coronarium*. Conversely, hco-miR167n and hco-miR393a have the opposite expression trend, leading to the preliminary hypothesis that these microRNAs may participate in the formation of volatile compounds by modulating the auxin-related signaling components *HcARF8* and *HcTIR1*. Moreover, it can be seen from Fig. 4 that the expression of miRNA and target genes present opposite expression patterns, which is consistent with the phenomenon of miRNA cutting on target genes.

Additionally, the target relationships between *HcARF8*-miR167n and *HcTIR1*-miR393a were confirmed using a tobacco transient expression system. The transient expression system was constructed to confirm that miRNAs degrade their target genes in vivo. Remarkably, in the experimental groups with pOx-hco-miR167n + PMS4-*HcARF8* and pOx-hco-miR393a + PMS4-*HcTIR1* constructs, only faint fluorescence was observed compared to the negative control groups comprising pOx-hco-miR167n + PMS4, pOx + PMS4-*HcARF8*, pOx-hco-miR393a + PMS4, and pOx + PMS4-*HcTIR1*, which displayed intense fluorescence (Fig. 5). This observation suggests that the miRNAs are effectively degrading their target genes in vivo. In summary, hco-miR393a and hco-miR167n respectively bind to *HcTIR1* and *HcARF8*, leading to mRNA degradation or translational repression. This further validates in vivo that *HcTIR1* and *HcARF8* are the target genes of hco-miR393a and hco-miR167n, respectively.

Table 2 Targets of *H. coronarium* miRNA identified by degradome sequencing

miRNA family	Target gene ID	Putative function
hco-miR156	comp46181_c0	callose synthase 3-like
	comp48189_c0	squamosa promoter-binding-like protein 16
	comp30142_c0	unknown
	comp27366_c0	homeobox-leucine zipper protein HOX16-like
	comp37992_c0	ATP-dependent zinc metalloprotease FTSH 2
	comp41926_c0	heptahelical transmembrane protein ADIPOR3-like
	comp48430_c0	ADP-ribosylation factor 1
hco-miR159	comp31174_c0	proteasome subunit beta type-5-like
	comp31186_c0	unknown
	comp47835_c0	transcription factor GA*MYB*-like
	comp47107_c0	uncharacterized LOC103983792
	comp49067_c0	protein plastid movement impaired 1-related 1
	comp35557_c0	FHA domain-containing protein FHA2-like
	comp40668_c0	protein DEK
	comp40625_c0	unknown
	comp46428_c0	heparanase-like protein 2
	comp43947_c0	glyoxysomal fatty acid beta-oxidation multifunctional protein MFP-a-like
hco-miR162	comp45610_c0	endoribonuclease Dicer homolog 1
hco-miR166	comp43255_c0	homeobox-leucine zipper protein HOX9
	comp42585_c0	serine/threonine-protein kinase STY46-like
	comp48810_c0	homeobox-leucine zipper protein HOX32-like
hco-miR167	comp47235_c0	uncharacterized LOC105049210
	comp45490_c0	auxin response factor 8-like ARF8
	comp42823_c0	unknown
	comp40432_c0	UDP-galactose transporter 1
	comp17573_c0	mitochondrial-processing peptidase subunit alpha-like
	comp96039_c0	unknown
hco-miR168	comp45501_c1	uncharacterized LOC109839632
hco-miR169	comp34201_c0	cystinosin homolog
hco-miR171	comp47960_c0	scarecrow-like protein 27
	comp45596_c0	scarecrow-like protein 15
	comp32225_c0	uncharacterized LOC103931388
	comp47572_c0	cyclin-dependent kinase G-2
hco-miR319	comp29930_c0	transcription factor TCP4
	comp45955_c1	transcription factor PCF5-like
	comp47835_c0	transcription factor GA*MYB*-like
	comp39846_c0	FRIGIDA-like protein 4a
	comp42681_c0	uncharacterized LOC103989154
hco-miR393	comp47036_c1	genome shotgun sequence
	comp44931_c0	protein DEK-like
	comp48815_c0	transport inhibitor response 1-like protein TIR1
	comp47879_c0	cellulose synthase-like protein H1
hco-miR394	comp47147_c0	uncharacterized LOC103984447
	comp48385_c1	F-box only protein 6
	comp48438_c0	phosphoinositide phosphatase SAC3
	comp16691_c0	tRNA (guanine(9)-N1)-methyltransferase
	comp34494_c1	laminin subunit alpha 3 (LAMA3)
	comp40642_c0	signal recognition particle subunit SRP72-like
	comp47501_c0	cyclin-dependent kinase F-3
hco-miR395	comp41552_c0	ATP sulfurylase 1, chloroplastic-like
	comp42239_c1	peroxidase 73
hco-miR396	comp30210_c0	40 S ribosomal protein S13
	comp43966_c1	CBL-interacting protein kinase 18-like

Table 2 (continued)

miRNA family	Target gene ID	Putative function
	comp46277_c0	DExH-box ATP-dependent RNA helicase DExH10
	comp48706_c0	oligopeptide transporter 7-like
	comp27123_c0	post-GPI attachment to proteins factor 3-like
	comp45123_c0	ABC transporter G family member 31
	comp41841_c0	RPM1-interacting protein 4
	comp68639_c0	alpha-galactosidase 1-like
hco-miR399	comp43073_c0	unknown
hco-miR408	comp36980_c2	whole genome shotgun sequence
	comp41984_c0	basic blue protein-like
hco-miR482	comp32217_c0	unknown
	comp40779_c0	TMV resistance protein N-like
	comp47696_c1	aspartyl protease 25
	comp41519_c0	splicing factor 3B subunit 2
hco-miR5179	comp41070_c0	APETALA3-like protein (AP3)
	comp45682_c0	uncharacterized LOC108953381
	comp48507_c0	AAA-ATPase At4g25835-like
hco-miR528	comp38590_c0	Japonica Group DNA, chromosome 2, cultivar: Nipponbare, complete sequence
	comp49773_c0	protein DMP2-like
hco-miR530	comp44896_c0	ABC transporter F family member 5
hco-miRn1	comp39725_c0	TIP4I-like family protein (TIP4I)
	comp45490_c0	auxin response factor 8-like
hco-miRn11	comp34044_c0	polygalacturonase-like
	comp39121_c1	chromosome Lu8
	comp49145_c0	transformation/transcription domain-associated protein-like
hco-miRn12	comp34044_c0	polygalacturonase-like
	comp39121_c1	chromosome Lu8
	comp49145_c0	transformation/transcription domain-associated protein-like
hco-miRn14	comp28588_c0	unknown
	comp34328_c0	ABC transporter A family member 7-like
	comp48561_c0	spermatogenesis-associated protein 20
hco-miRn15	comp44913_c0	18 S ribosomal RNA gene
hco-miRn19	comp38703_c0	acyl-CoA-binding domain-containing protein 3-like
hco-miRn21	comp38688_c0	hypothetical protein
	comp37459_c0	unknown
hco-miRn24	comp36980_c2	whole genome shotgun sequence
hco-miRn31	comp28405_c0	annexin D4-like
	comp45540_c0	activating signal cointegrator 1
hco-miRn32	comp27938_c0	unknown
	comp43835_c0	uncharacterized LOC105051789
hco-miRn4	comp23808_c0	threonine dehydratase biosynthetic, chloroplastic
	comp36577_c0	ASC1-like protein 3
	comp45224_c0	Serine-rich protein

Changes in volatile fragrance compounds contents and gene expression in *H. coronarium* after exogenous IAA and PCIB treatments

HcARF8 and *HcTIR1* are two pivotal signaling components in the auxin response pathway, and exogenous applications of IAA and the auxin inhibitor PCIB were found to impact the emission of volatile aroma compounds in *H. coronarium*. The results showed that after 0.1 mM IAA treatment of *H. coronarium*, the contents of ocimene, eucalyptol and allo-ocimene, as well as the expression levels of hco-miR167n and hco-miR393a, significantly increased, whereas methyl benzoate content notably decreased ($p < 0.05$). Conversely, upon treatment with 350 mg/L PCIB, the concentrations of ocimene, linalool, allo-ocimene, and methyl benzoate, as well as the expression of hco-miR167n, hco-miR393a, *HcARF8*, and *HcTIR1*, were all significantly reduced (Fig. 6). These findings suggest that hco-miR167n and hco-miR393a can be regulated by exogenous auxin and further confirm that *HcARF8* and *HcTIR1*, as targets of hco-miR167n and

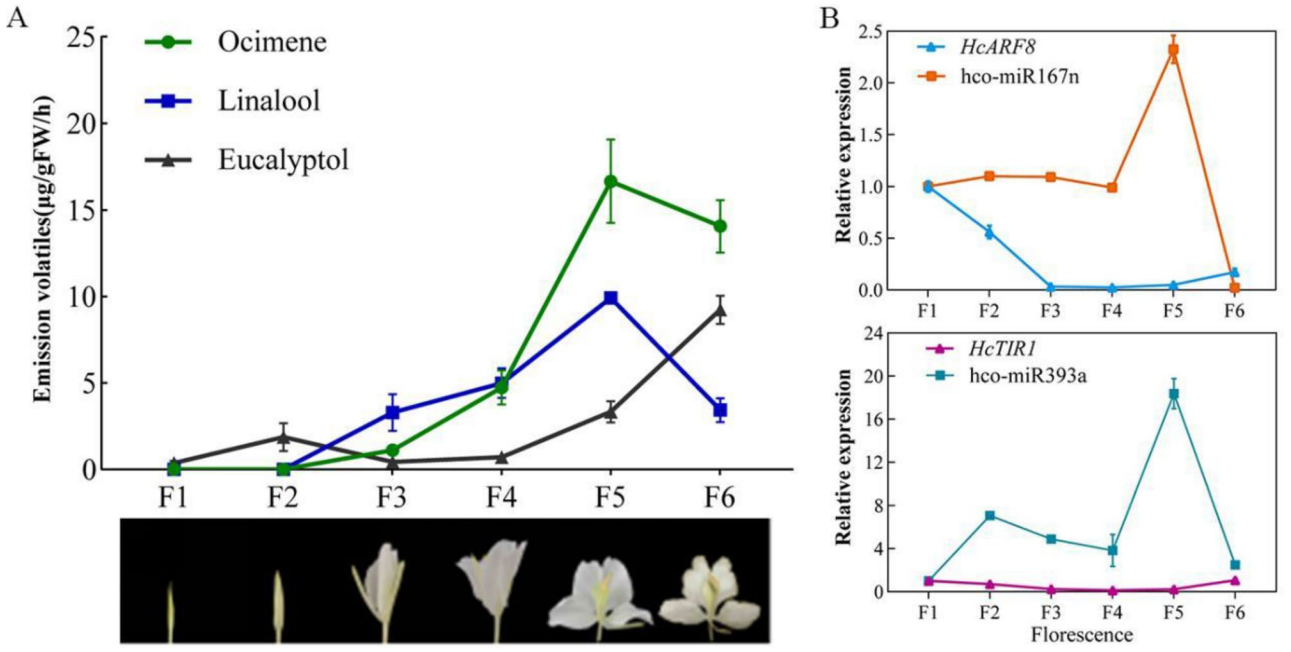

Fig. 4 Dynamics of volatile aroma compounds and the relative expression of *HcARF8*-miR167n and *HcTIR1*-miR393a

hco-miR393a respectively, indirectly modulate the synthesis and release of aroma compounds in *H. coronarium*.

Functional validation of *HcARF8*-miR167n and *HcTIR1*-miR393a in *H. coronarium*

Short tandem target mimic (STTM) technology is an effective technique for silencing microRNAs (miRNAs) and has been successfully applied in plants [27]. After STTM to interfere with hco-miR167n and hco-miR393a, the flower aroma compounds such as ocimene, linalool, myrcene, and methyl benzoate decreased significantly compared with the control (Fig. 7A). To further analyze the expression changes of related genes after STTM interference with hco-miR167n and hco-miR393a, qRT-PCR was employed. The results showed that after transient overexpression interfered with hco-miR167n, the expression of *HcARF8* increased, while the expression of terpene synthase genes *HcTPS8*, *HcTPS10*, and methyl benzoate synthase gene *HcBSMT1* decreased significantly compared with the control (Fig. 7B, D). However, after transient overexpression interfered with hco-miR393a, the expression of *HcTIR1* decreased, and the expression of terpene synthase gene *HcTPS3*, *HcTPS5*, and methyl benzoate synthase gene *HcBSMT2* decreased significantly compared with the control (Fig. 7C, D). The results further showed that *HcARF8* and *HcTIR1* were the target genes of hco-miR167n and hco-miR393a respectively, and hco-miR167n and hco-miR393a were positive regulators of flower aroma compounds in *H. coronarium*.

After VIGS *HcARF8*, the contents of linalool and methyl benzoate increased significantly, while the contents of ocimene and eucalyptol decreased significantly. After VIGS *HcTIR1*, the content of linalool increased significantly, while the content of eucalyptol decreased significantly (Fig. 8A). To further analyze the expression changes of related genes after VIGS *HcARF8* and *HcTIR1*, qRT-PCR was employed. The results showed that after silencing *HcARF8*, the expression of terpene synthase gene *HcTPS1*, *HcTPS3*, *HcTPS5* and *HcTPS10* increased significantly, while the expression of methyl benzoate synthase gene *HcBSMT2* decreased significantly compared with the control (Fig. 8B, D). However, after silencing *HcTIR1*, the expression of terpene synthase genes *HcTPS1*, *HcTPS3*, *HcTPS5*, *HcTPS8*, *HcTPS10* and methyl benzoate synthase gene *HcBSMT1* increased significantly (Fig. 8C, D). The above results suggest that *HcARF8* and *HcTIR1* may be negative regulators of flower aroma compounds.

Transcriptional activity analysis of *HcARF8* on key genes involved in aroma compounds synthesis

To further elucidate the transcriptional regulation of *HcARF8* on the synthase genes involved in *H. coronarium* aroma compounds synthesis, CaMV35S-*HcARF8* vector and *HcTPS8/HcTPS5/HcTPS8pro*-LUC/CaMV35S-REN vector were constructed and transferred into *A. tumefaciens* (EHA105), respectively. After infecting tobacco leaf cells, the LUC and REN activity were detected. Compared to the CaMV35S-empty vector control group, the expression of the LUC reporter gene driven by the *HcTPS8* promoter was significantly reduced in the CaMV35S-*HcARF8* transformed group, with the expression level in

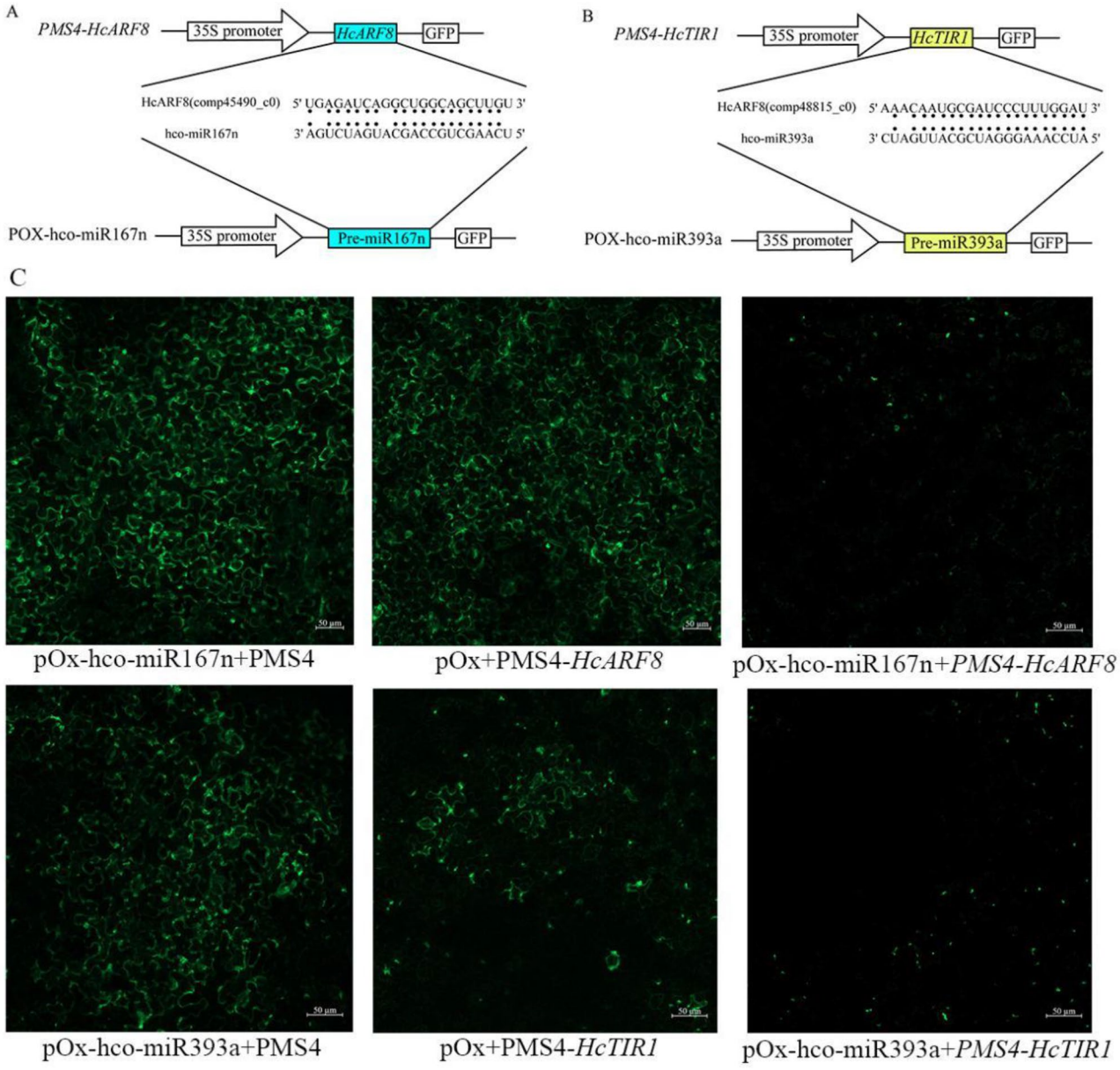

Fig. 5 Tobacco co-transformation assay to validate the targeting of *HcARF8* by miR167n and *HcTIR1* by miR393a. **A**, Schematic diagram of the *PMS4-HcARF8* and pOx-hco-miR167n construct for vector assembly. **B**, Schematic diagram of the *PMS4- HcTIR1* and pOx-hco- miR393a construct for vector assembly. **C**, Fluorescence images of each group

the control group being 3.45 times higher (Fig. 9A, B). Moreover, *HcTPS3/5/8pro*-pAbAi vector and *HcARF8*-pGADT7 vector were constructed respectively, and the interaction between *HcARF8* and *HcTPS*3/5/8 promoter was verified by yeast one-hybrid assays. The yeast cells transformed with *HcARF8* along with *HcTPS38pro*-pAbAi were capable of growth on medium containing AbA (300 ng/mL), whereas yeast cells transformed with the empty vector control pGADT7 remained unable to grow on AbA-containing plates (Fig. 9C). Collectively, these findings indicate that the transcription factor *HcARF8* can bind to the promoter of *HcTPS8* and transcriptionally inhibit its expression, thereby participating in the regulation of terpenoid volatile aroma compound biosynthesis in *H. coronarium*.

Discussion

MicroRNAs (miRNAs) are a class of non-coding small RNA molecules that regulate gene expression by targeting mRNAs and inhibiting their translation, thereby controlling gene expression at the transcriptional or post-transcriptional level [28]. In recent years, increasing evidence has shown that miRNAs play significant roles in regulating the synthesis of plant secondary metabolites.

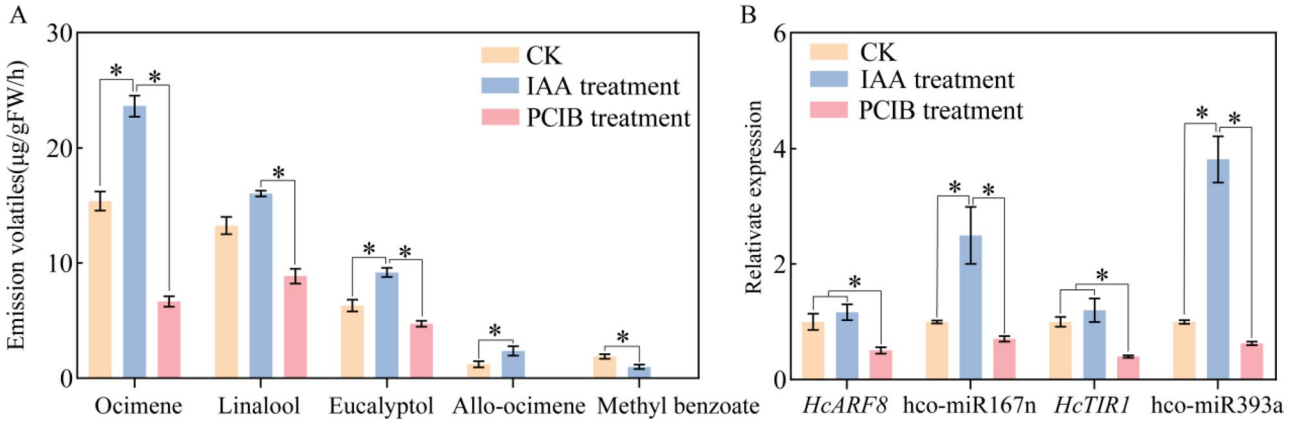

Fig. 6 Aroma volatilization and related gene expression after exogenous IAA and PCIB treatment. * P value < 0.05 (Student's t-test)

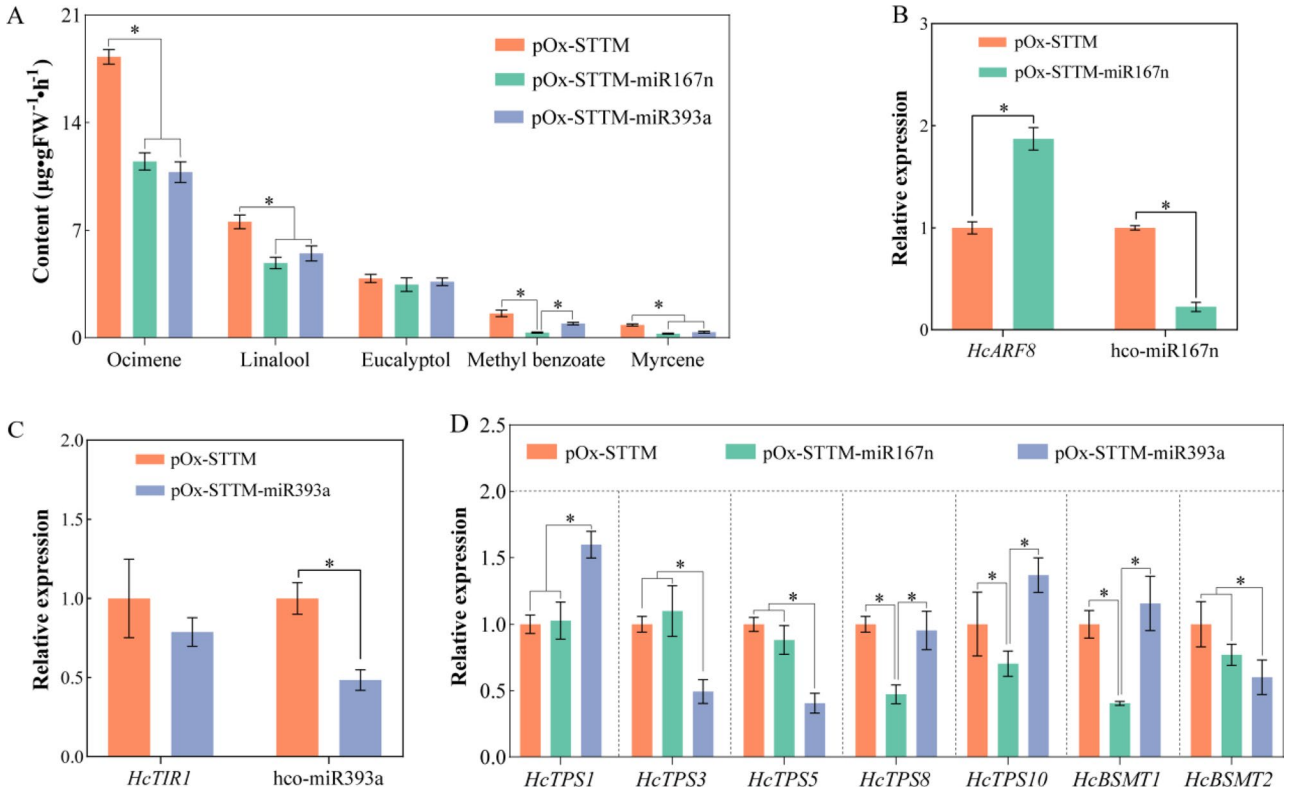

Fig. 7 STTM interfered with aroma volatilization and related gene expression after hco-miR167n and hco-miR393a

Through small RNA and degradome sequencing technologies, various miRNAs involved in secondary metabolite biosynthesis have been identified in multiple plant species, including miR160 [29], miR156 [30], and miR4995 [31]. In *Arabidopsis thaliana*, miR858a targets *MYBL2*, thereby regulating the expression of chalcone synthase (CHS), chalcone isomerase (CHI), and flavonoid 3-hydroxylase (F3H) to modulate anthocyanin accumulation [32]. In *Gerbera hybrida*, Ghy-miRn75 targets the bHLH transporter *GMYC1*, which binds to the promoter of *GMYB10* and activates *GDFR2*, thus regulating anthocyanin biosynthesis [33]. With the continuous development of high-throughput sequencing technology, bioinformatics algorithms and sequencing methods have been widely applied, leading to the discovery of an increasing number of plant miRNAs involved in the regulation of secondary metabolite biosynthesis. Researchers performed miRNA sequencing on the petals of *Rosa rugosa* and identified 383 conserved miRNAs and 625 novel miRNAs, among which 53 miRNAs were differentially expressed in the highly fragrant variety *R. rugosa* 'White Purple Branch' [34]. In this study, we performed

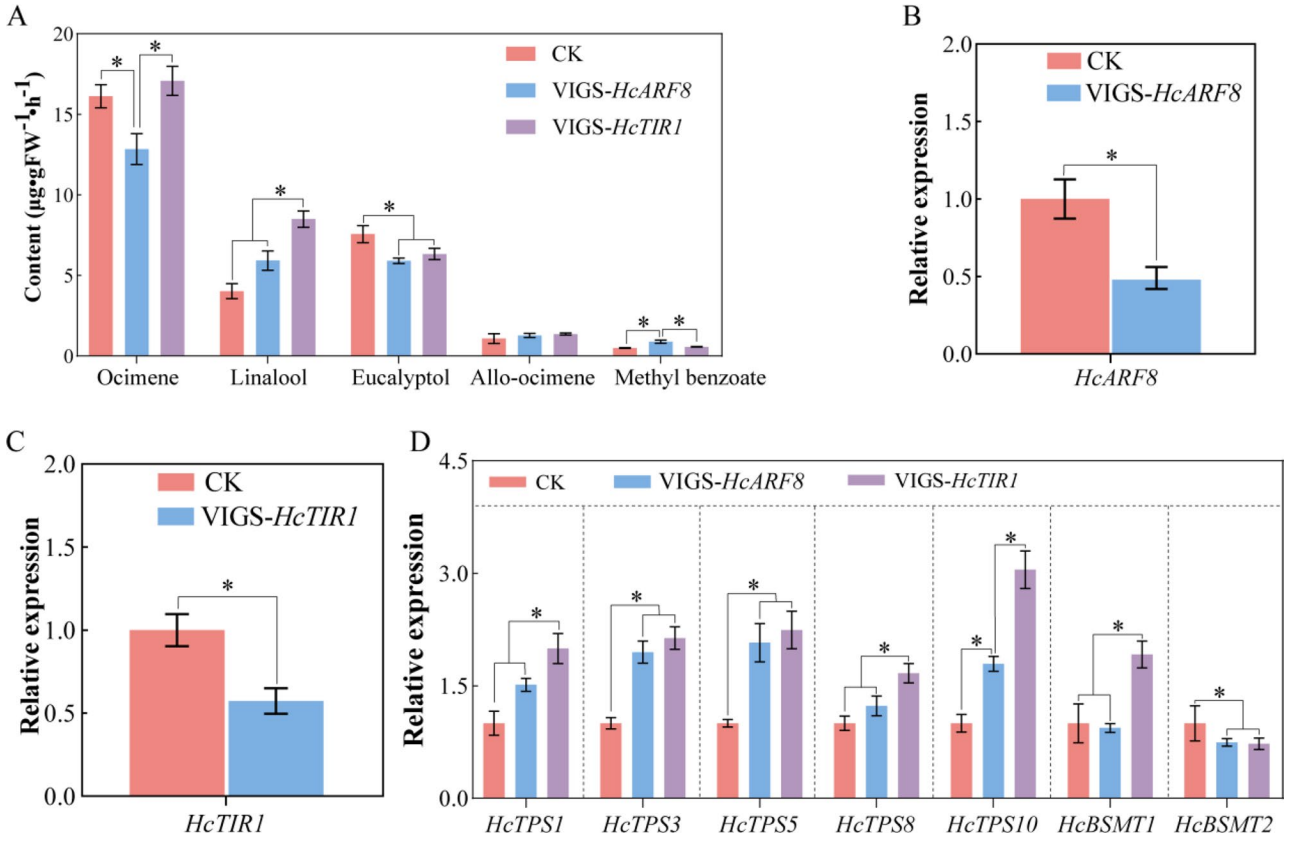

Fig. 8 Aroma volatilization and related gene expression after VIGS *HcARF8* and *HcTIR1*

small RNA sequencing on petals of *H. coronarium* at different developmental stages, identifying 171 known miRNAs and 32 specific miRNAs belonging to 24 distinct miRNA families. Further analysis revealed that several miRNA families (such as hco-miR156, hco-miR166, hco-miR167, hco-miR408, and hco-miR396) exhibited significantly high expression levels at the F1, F5, or F6 stages, which is consistent with previous findings in *Gerbera hybrida* [33] and *Osmanthus fragrans* [35]. Accumulating evidence has established the miR156-SPL module as a conserved flowering timing hub across plant species. In *Arabidopsis thaliana*, miR156 negatively regulates FLOWERING LOCUS T (FT) expression through post-transcriptional repression of SPL9 [36], while in Oryza sativa, OsmiR156 modulates plant architecture and floral transition via the OsSPL14-IPA1 regulatory cascade [37]. These findings strongly suggest that miR156 may orchestrate the coordinated regulation of flowering and fragrance biosynthesis in *H. coronarium* through distinct downstream targets. While these observations provide crucial insights into the miR156-mediated flowering-fragrance regulatory network, the precise molecular mechanisms underlying this coordination in Zingiberaceae species remain to be fully elucidated.

Additionally, we found that the majority of sRNAs in *H. coronarium* were 24 nucleotides in length, which is similar to the sRNA length distribution in *Lilium davidii* var. *unicolor* [38] and *Phaseolus vulgaris* L [39]. However, this distribution differed from that observed in *Canna* [40] and *Brassica juncea* [41], suggesting that the sRNA length distribution may vary across different plant species. These results not only validate the widespread role of miRNAs in plant secondary metabolism but also provide new insights into the regulation of fragrance in crops such as *H. coronarium*. The regulation of secondary metabolite biosynthesis by miRNAs may be a universal mechanism with significant implications for plant growth, development, environmental adaptability, and the production of volatile compounds. Future research could further explore the specific roles of these miRNAs in the regulation of fragrance metabolism in *H. coronarium* and uncover how miRNAs interact with other signaling pathways to collectively regulate fragrance synthesis and its biological functions.

To further investigate the role of miRNAs in the regulation of fragrance in *H. coronarium*, it is essential to analyze the miRNAs and their potential target genes. In this study, we identified differentially expressed miRNAs and monitored the transcriptional changes at different developmental stages of *H. coronarium*, revealing the diverse functions of miRNAs in its development. A total of 122 differentially expressed miRNAs were identified across

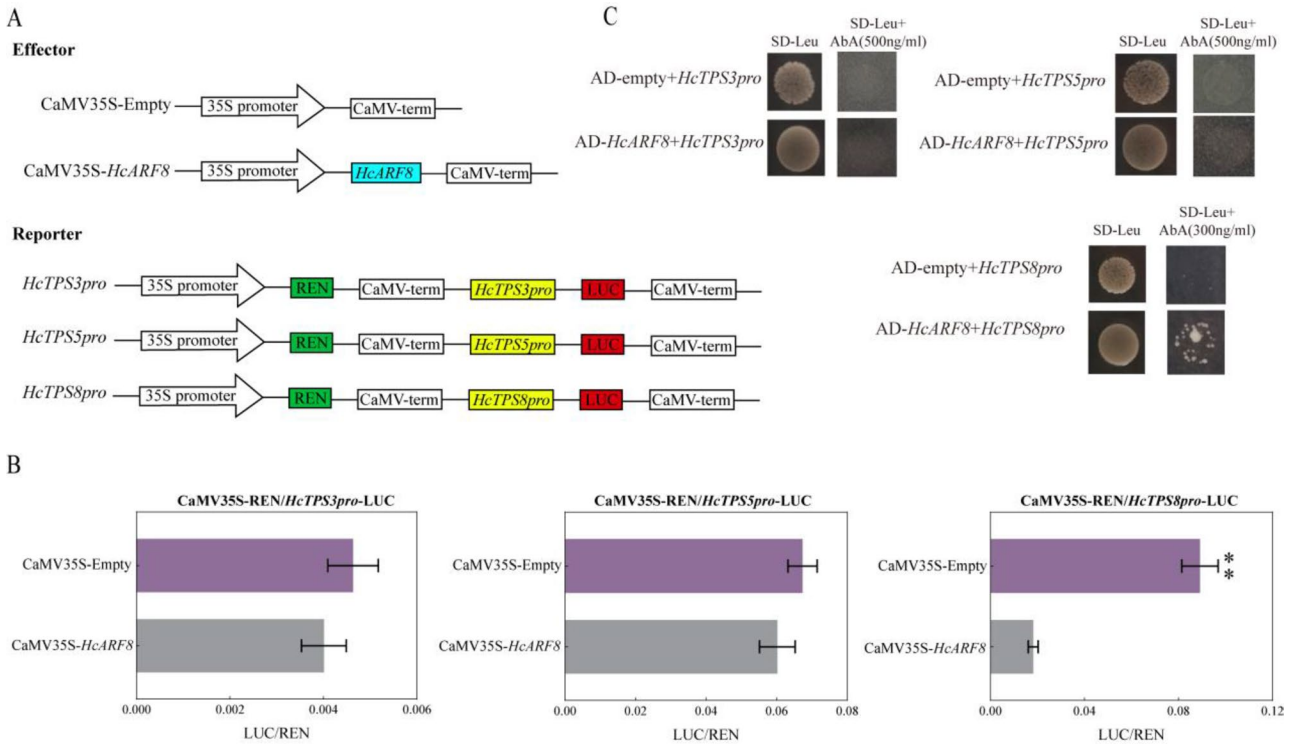

Fig. 9 *HcARF8* specifically targets the *HcTPS8* promoter. **A**, Diagrams of the reporter and effector constructs used for the dual-LUC transient expression assay; **B**, LUC assay showing the activation of the *HcTPS3/5/8* promoters by *HcARF8*. The LUC/REN ratio reflects transactivation activity. Data are presented as the mean ± SD ($n = 3$). ** $P < 0.01$; **C**, Y1H analysis of *HcARF8* binding to the *HcTPS3/5/8* promoter

three comparison groups, with a significantly higher number of upregulated miRNAs than downregulated ones (Fig. 3). This finding suggests that miRNAs may be involved in various biological processes and regulatory mechanisms during the development of *H. coronarium*. Furthermore, these differentially expressed miRNAs exhibited significantly different expression patterns at different developmental stages, indicating that they have stage-specific and complex regulatory roles in *H. coronarium* development. This result is consistent with previous findings in other plants, such as *Gerbera hybrida* and *Osmanthus fragrans*, which also revealed the important roles of miRNAs in plant development [33, 35]. Based on miRNA research in *Arabidopsis thaliana* and other species, we further predicted 90 potential target genes from 30 miRNA families (Table 2). Many of these target genes belong to regulatory element families, such as *GAMYB* transcription factors, TCP4 transcription factors, auxin receptors TIR and ARF, and scarecrow-like proteins, which regulate the expression of other genes during plant growth, development, and responses to biotic or abiotic stress [42, 43]. Among these, hco-miR159 targets the most genes, with 10 target genes, reflecting the high conservation of hco-miR159. This result is consistent with studies in *Lilium davidii* var. *unicolor*, which indicated that miR159 is one of the largest and most conserved miRNA families [38]. As an ancient miRNA family, the diversity among its members may have arisen from gene mutations induced by environmental factors during plant evolution, suggesting that the miR159 family may exhibit some degree of evolutionary diversity [44]. This finding further enhances our understanding of the diversity of miRNAs and their potential regulatory mechanisms in the fragrance metabolism of *H. coronarium*. This study not only provides new insights into the miRNA network involved in the regulation of fragrance in *H. coronarium* but also lays the foundation for future functional studies of miRNAs in*H. coronarium* and other Zingiberaceae species. These findings offer valuable clues for further exploring the role of miRNAs in the synthesis of plant secondary metabolites, particularly in the specific mechanisms involved in plant fragrance synthesis.

Plant hormones, as components of signaling pathways, play crucial roles in the synthesis of secondary metabolites and plant stress tolerance. In this study, we found that hco-miR167, hco-miR171, and hco-miR393 target *HcARF8*, *HcSCR15*, and *HcTIR1*, respectively, and are involved in plant hormone signaling pathways (Table 2). These miRNAs may indirectly influence key steps in the volatile metabolism of *H. coronarium* by regulating the expression of these target genes. The main volatile compounds in the scent of *H. coronarium* are eucalyptol, ocimene, and linalool, and their volatile emissions increase as the flowers open, peaking at the F5 stage, and

slightly decrease as the flowers age. This variation may be closely related to the regulatory roles of miRNAs at different stages of flower development. The application of exogenous auxin plays a key role in regulating the synthesis and accumulation of various secondary metabolites. In this study, IAA treatment significantly increased the levels of ocimene, eucalyptol, and allo-ocimene in *H. coronarium*, while PCIB treatment significantly reduced the levels of ocimene, linalool, allo-ocimene, and methyl benzoate. These results indicate that auxin plays an important role in regulating the release of floral scent compounds in *H. coronarium*, consistent with the findings of Ke et al. [23]. Furthermore, the impact of environmental factors (such as temperature, humidity, and light intensity) and other plant hormones (such as gibberellin and cytokinins) on miRNA regulation warrants further investigation. For example, combined treatments with environmental stresses or hormones may alter miRNA expression patterns, which could, in turn, affect the synthesis and release of scent compounds in *H. coronarium*. Therefore, future research should focus on the interaction between miRNA regulation, environmental conditions, and hormones to provide a comprehensive understanding of the mechanisms underlying floral scent regulation in *H. coronarium*.

In plants, ARF and TIR genes have been extensively studied, particularly the regulatory modules involving miR167-ARF and miR393-TIR, which play crucial roles in flower development, root formation, and stress responses such as salt and drought tolerance. However, the role of these two regulatory modules in flower fragrance formation remains limited. In this study, by combining high-throughput miRNA sequencing and degradome sequencing analyses, we found that auxin-related genes *HcARF8* and *HcTIR1* in *H. coronarium* are regulated by hco-miR167n and hco-miR393a, revealing a new mechanism of miRNA regulation in flower fragrance. The miR167 family is a conserved group of microRNAs in plants, which mainly regulate the ARF gene family to influence the auxin signaling pathway, thereby regulating various aspects of plant growth and development. Duan et al. [42] studied miR167 in tomato and found that STTM-miR167a, by increasing the expression of *SlARF6* and *SlARF8*, altered the levels of carotenoids and lycopene, thereby delaying fruit ripening and senescence. Gutierrez et al. [43] discovered that in *Arabidopsis*, miR167 targets ARF6 and ARF8, which are involved in auxin signaling and positively regulate adventitious root formation. These studies indicate that miR167 plays an important role in plant growth and development by regulating ARF genes. However, the role of miR167 in fragrance regulation is still not fully understood. In our study, qRT-PCR showed that hco-miR167n and *HcARF8* exhibit opposite expression trends. Tobacco co-transformation experiments revealed that hco-miR167n can bind to *HcARF8*, leading to mRNA degradation or inhibition of translation. STTM experiments suggested that miR167 may regulate the accumulation of fragrance compounds by modulating ARF genes. Additionally, miR393 is known to participate in auxin signaling in rice by regulating the miR156-IPA1-miR408-5p-IAA30 module [45]. In this study, we also found that hco-miR393a regulates the expression of *HcTIR1*, suggesting that miR393 may play a role in the production of fragrance in *H. coronarium*. Analysis of STTM and VIGS experiments revealed that both hco-miR167n and hco-miR393a positively regulate fragrance metabolism, while *HcARF8* and *HcTIR1* act as negative regulators in the accumulation of fragrance compounds. These results are consistent with previous studies and further support the role of miR167 and miR393 as regulators in plant hormone signaling pathways. TIR1 and ARF8 have been confirmed as target genes of miR393 and miR167, and are involved in plant hormone responses [46, 47]. Furthermore, after IAA treatment, the expression of hco-miR167n and hco-miR393a significantly increased, suggesting that these miRNAs may influence fragrance metabolism accumulation through the regulation of environmental signals. These findings uncover a new mechanism for the regulation of fragrance in *H. coronarium* and provide new insights for breeding programs aimed at enhancing flower fragrance through genetic modification.

In *H. coronarium*, the formation of floral fragrance is one of its most important characteristics. The plant is widely used in horticultural landscapes and the cut flower market due to its intense fragrance and vibrant flower color. The primary fragrance components are terpenoid compounds, which are the most diverse class of aroma compounds, exhibiting structural variations and differences in the number of isoprene units. These compounds are typically categorized into monoterpenes, sesquiterpenes, and diterpenes. Terpene synthases (TPS) play a crucial role in the biosynthesis of terpenoid compounds, particularly in the final stage of synthesis, where TPS catalyzes the conversion of substrates such as GPP, FPP, and GGPP into specific terpenoids [48]. Recent studies have also highlighted the regulatory role of miRNAs in the synthesis of floral fragrance compounds in plants. The miR156 family targets SPL genes, and SPL9 directly binds to the promoter of *AtTPS21* in *Arabidopsis*, activating its expression and regulating the release of sesquiterpenes during floral development [49]. However, it remains unclear whether miRNAs in *H. coronarium* regulate fragrance release by targeting related genes. To address this, we conducted dual-luciferase reporter assays and yeast one-hybrid experiments using the promoters of *HcARF8* and *HcTPS* genes to explore the potential role of

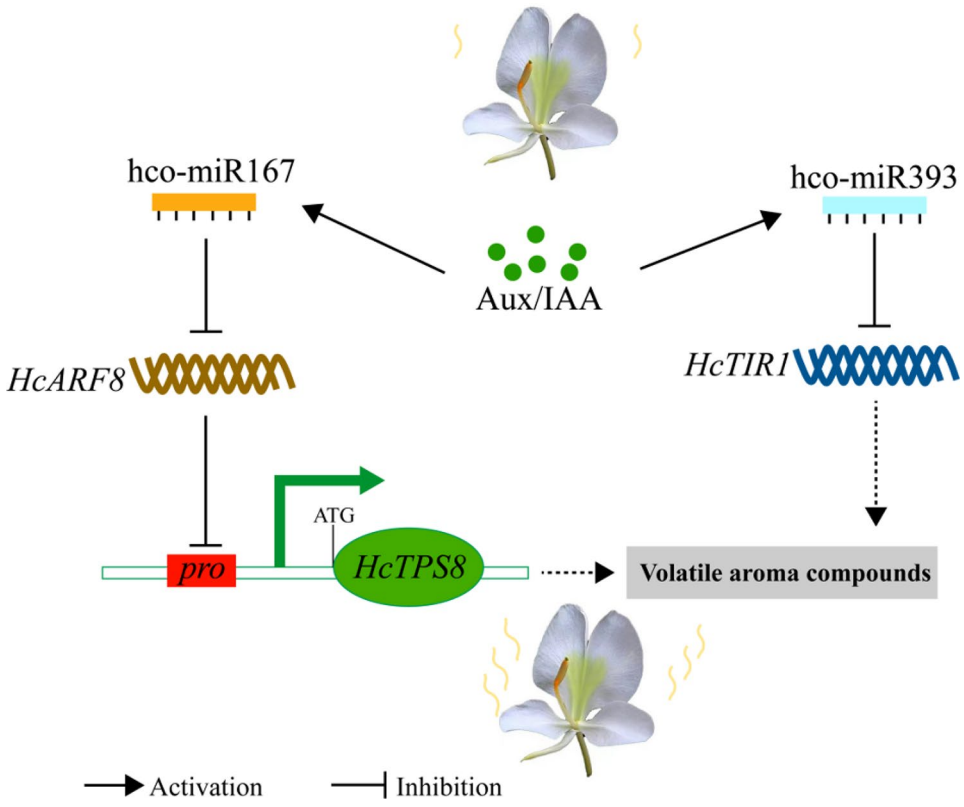

Fig. 10 The regulatory network diagram of *HcARF8*-miR167n and *HcTIR1*-miR393a regulating the synthesis of volatile aroma compounds in *H. coronariu*

miRNAs in regulating floral fragrance in *H. coronarium*. The results indicate that *HcARF8* binds to the promoter of *HcTPS8* and activates its transcription, thereby regulating terpenoid biosynthesis in *H. coronarium* (Fig. 9). Using high-throughput sequencing technology combined with molecular biology techniques, this study reveals for the first time the miRNA regulatory network in *H. coronarium*. The findings demonstrate that these miRNAs regulate the release of fragrance compounds by targeting key genes. Building on our previous research, we further propose a miRNA regulatory network in *H. coronarium* (Fig. 10). Specifically, hco-miR167 targets and degrades *HcARF8*, thereby inhibiting its binding to the *HcTPS8* promoter and repressing *HcTPS8* transcription. Additionally, hco-miR393a targets the auxin receptor *HcTIR1* and indirectly affects the synthesis of floral fragrance compounds in *H. coronarium*. These results provide new insights into the molecular mechanisms underlying floral fragrance regulation in *H. coronarium* and offer theoretical support for horticultural improvements aimed at enhancing fragrance quality by modulating the miRNA network. Future research could further investigate the interactions between miRNAs and other genes, as well as their role in the fragrance biosynthesis pathway, thereby contributing more insights into plant aroma regulation.

This study validated the regulatory relationships between specific miRNAs and their target genes in *H. coronarium*; however, many predicted target genes have yet to be functionally confirmed. Future research should incorporate additional functional validation approaches, such as CRISPR-Cas9-mediated gene knockout, to precisely elucidate the roles of miRNAs and their target genes in floral fragrance metabolism. Moreover, we observed that exogenous IAA and PCIB treatments influenced miRNA expression and the biosynthesis of floral volatile compounds in *H. coronarium*. However, the regulatory mechanisms of plant hormones are highly complex, and IAA may interact with other hormones, such as jasmonic acid and abscisic acid, thereby affecting miRNA-mediated regulation. Therefore, future studies should further investigate the crosstalk among different phytohormones to gain deeper insights into the regulatory role of miRNAs within the plant hormone signaling network.

Conclusion

This study identified that the volatile emissions of the primary floral fragrance compounds eucalyptol, ocimene, and linalool in *H. coronarium* increase continuously as the flower opens. Across different developmental stages of *H. coronarium*, 171 conserved miRNAs from 24

miRNA families and 32 novel miRNAs were identified using high-throughput sRNA sequencing. Degradome sequencing revealed 102 mRNA degradation sites corresponding to 90 target genes from 30 miRNA families. Exogenous treatments with IAA and the auxin inhibitor PCIB were found to affect the release of floral fragrance compounds in *H. coronarium*. Molecular biology experiments confirmed that hco-miR167n and hco-miR393a act as positive regulators of floral fragrance metabolism in *H. coronarium*, while *HcARF8* and *HcTIR1* act as negative regulators. Specifically, *HcARF8* binds to the promoter of the terpene synthase *HcTPS8*, thereby regulating the synthesis of floral fragrance compounds. In conclusion, this study utilized high-throughput small RNA sequencing for the first time to identify miRNAs in *H. coronarium*, laying the foundation for research on miRNA-mediated regulation of floral fragrance and terpenoid biosynthesis. Furthermore, by modulating miRNAs or their target genes involved in terpenoid compound regulation, it may be possible to enhance the accumulation of these compounds, offering new avenues for improving plant fragrance.

Supplementary Information

The online version contains supplementary material available at https://doi.org/10.1186/s12864-025-11583-0.

Supplementary Material 1

Supplementary Material 2

Acknowledgements
This work was supported by the Rural Revitalization Strategy of Guangdong Province.

Author contributions
Y.P.F.designed and conceived the experiment. F.W. wrote the paper. F.W. and L.L. carried out the experiments and analyzed the data. R.C.Y. and X.L. conducted the resource survey. X.Y.L.,Y.Y.Y. and Y.C.Y. supervised and managed the experiment. Y.P.F. and R.C.Y. revised the manuscript.

Funding
This work was financially supported by the Rural Revitalization Strategy of Guangdong Province(Grant No.2022-NPY-00-042).

Data availability
All data generated or analyzed during this study are included in this published article and its supplementary information files. The datasets generated during the current study are available in the SRA database of the National Center for Biotechnology Information (NCBI) system with accession number of PRJNA1244539 and PRJNA1244583.

Declarations

Ethics approval and consent to participate
Not applicable.

Consent for publication
Not applicable.

Competing interests
The authors declare no competing interests.

Received: 16 August 2024 / Accepted: 8 April 2025
Published online: 30 April 2025

References

1. Minow MA, Coneva V, Lesy V, Misyura M, Colasanti J. Plant gene Silencing signals move from the phloem to influence gene expression in shoot apical meristems. BMC Plant Biol. 2022;22(1):606.
2. Bai S, Tian Y, Tan C, Bai S, Hao J, Hasi A. Genome-wide identification of MicroRNAs involved in the regulation of fruit ripening and climacteric stages in melon (*Cucumis melo*). Hortic Res. 2020;7:106.
3. Moran Y, Fredman D, Praher D, Li XZ, Wee LM, Rentzsch F, Zamore PD, Technau U, Seitz H. Cnidarian MicroRNAs frequently regulate targets by cleavage. Genome Res. 2014;24(4):651–63.
4. Tang YY, Liu HH, Guo SY, Wang B, Li ZT, Chong K, Xu YY. OsmiR396d affects Gibberellin and brassinosteroid signaling to regulate plant architecture in rice. Plant Physiol. 2017;176(1):946–59.
5. Cai JH, Wu ZL, Hao YW, Liu YL, Song ZY, Chen WX, Li XP, Zhu XY. Small RNAs, degradome, and transcriptome sequencing provide insights into Papaya fruit ripening regulated by 1-MCP. Foods. 2021;10(7):1643.
6. Dai XH, Lu Q, Wang J, Wang LL, Xiang FN, Liu ZH. MiR160 and its target genes ARF10, ARF16 and ARF17 modulate hypocotyl elongation in a light, BRZ, or PAC-dependent manner in *Arabidopsis*: miR160 promotes hypocotyl elongation. Plant Sci. 2021;303:110686.
7. Li J, Wang YZ, Zhang YX, Wang WY, Irish VF, Huang TB. RABBIT EARS regulates the transcription of TCP4 during petal development in *Arabidopsis*. J Exp Bot. 2016;67(22):6473–80.
8. Lian JP, Yuan C, Feng YZ, Liu Q, Wang CY, Zhou YF, Huang QJ, Zhu QF, Zhang YC, Chen YQ, Yu Y. MicroRNA397 promotes rice flowering by regulating the photorespiration pathway. Plant Physiol. 2023;194(4):2101–16.
9. Jerome Jeyakumar JM, Wang AA, Thiruvengadam WM, M. Characterizing the role of the miR156-SPL network in plant development and stress response. Plants. 2020;9(9):1206.
10. Millar AA, Lohe A, Wong GG. Biology and function of miR159 in plants. Plants. 2019;8(8):255.
11. Sang Q, Vayssières A, Ó'Maoiléidigh DS, Yang X, Vincent C, de Bertran Garcia E, Cerise M, Franzen R, Coupland G. MicroRNA172 controls inflorescence meristem size through regulation of APETALA2 in *Arabidopsis*. New Phytol. 2022;235(1):356–71.
12. Baker CC, Sieber P, Wellmer F, Meyerowitz EM. The early extra petals1 mutant uncovers a role for MicroRNA miR164c in regulating petal number in *Arabidopsis*. Curr Biol. 2005;15:303–15.
13. Hou CY, Wu MT, Lu SH, Hsing YI, Chen HM. Beyond cleaved small RNA targets: unraveling the complexity of plant RNA degradome data. BMC Genomic. 2014;15:15.
14. Addo-Quaye C, Eshoo TW, Bartel DP, Axtell MJ. Endogenous SiRNA and MiRNA targets identified by sequencing of the *Arabidopsis* degradome. Curr Biol. 2008;18(10):758–62.
15. Sun ZT, He YQ, Li JM, Wang X, Chen JP. Genome-wide characterization of rice black streaked Dwarf virus-responsive MicroRNAs in rice leaves and roots by small RNA and degradome sequencing. Plant Cell Physiol. 2015;56(4):688–99.
16. Zhao YP, Xu ZH, Mo QC, Zou C, Li WX, Xu YB, Xie CX. Combined small RNA and degradome sequencing reveals novel MiRNAs and their targets in response to low nitrate availability in maize. Ann Bot. 2013;112(3):633–42.
17. Kim JE, Park JH, Lim CJ, Lim JY, Ryu JY, Lee BW, Choi JP, Kim WB, Lee HY, Choi YR. Small RNA and transcriptome deep sequencing proffers insight into floral gene regulation in *Rosa* cultivars. BMC Genomics. 2012;13:657.
18. Jin QJ, Xue ZY, Dong CL, Wang YJ, Chu LL, Xu YC. Identification and characterization of MicroRNAs from tree peony (*Paeonia ostii*) and their response to copper stress. PLoS ONE. 2015;10(2):e0117584.
19. Ma L, Zhou L, Quan SW, Xu H, Yang JP, Niu JX. Integrated analysis of mRNA-seq and miRNA-seq in calyx abscission zone of Korla fragrant Pear involved in calyx persistence. BMC Plant Biol. 2019;19:1–18.
20. Jodder J. miRNA-mediated regulation of auxin signaling pathway during plant development and stress responses. J Biosci. 2020;45:91.
21. Wu, M. F., Tian, Q., Reed, J. W., 2006. Arabidopsis microRNA167 controls patterns of ARF6 and ARF8 expression, and regulates both female and male reproduction. Development, 21, 4211–4218
22. Iglesias MJ, Terrile MC, Windels D, Lombardo MC, Bartoli CG, Vazquez F, Estelle M, Casalongué CA. MiR393 regulation of auxin signaling and redox-related

components during acclimation to salinity in *Arabidopsis*. PLoS ONE. 2014;9(9):e107678.
23. Ke YG, Abbas F, Zhou YW, Yu RC, Fan YP. Auxin-responsive R2R3-MYB transcription factors HcMYB1 and HcMYB2 activate volatile biosynthesis in *Hedychium coronarium* flowers. Front Plant Sci. 2021;12:710826.
24. Yue YC, Yu RC, Fan YP. Characterization of two monoterpene synthases involved in floral scent formation in *Hedychium coronarium*. Planta. 2014;240(4):745–62.
25. Zhou, Y., Abbas, F., Wang, Z., Yu, Y., Yue, Y., Li, X., Yu, R., Fan, Y., 2021. HS–SPME–GC–MS and Electronic Nose Reveal Differences in the Volatile Profiles of Hedychium Flowers. Molecules 2021, 26, 5425.
26. Niemeyer M, Moreno Castillo E, Ihling CH, Iacobucci C, Wilde V, Hellmuth A, Hoehenwarter W, Samodelov SL, Zurbriggen MD, Kastritis PL. Flexibility of intrinsically disordered degrons in AUX/IAA proteins reinforces auxin co-receptor assemblies. Nat Commun. 2020;11(1):2277.
27. Wang C, He XW, Wang XX, Zhang SX, Guo XQ. ghr-miR5272a-mediated regulation of GhMKK6 gene transcription contributes to the immune response in cotton. J Exp Bot. 2017;68(21–22):5895–906.
28. Djami-Tchatchou AT, Sanan-Mishra N, Ntushelo K, Dubery IA. Functional roles of MicroRNAs in agronomically important plants—potential as targets for crop improvement and protection. Front Plant Sci. 2017;8:378.
29. Wu B, Li Y, Yan HX, Ma YM, Luo HM, Yuan LC, Chen SL, Lu SF. Comprehensive transcriptome analysis reveals novel genes involved in cardiac glycoside biosynthesis and MlncRNAs associated with secondary metabolism and stress response in *Digitalis purpurea*. BMC Genomics. 2012;13:1–22.
30. Fan K, Fan DM, Ding ZT, Su YH, Wang XC. Cs-miR156 is involved in the nitrogen form regulation of catechins accumulation in tea plant (*Camellia sinensis* L). Plant Physiol Biochem. 2015;97:350–60.
31. Vashisht I, Mishra P, Pal T, Chanumolu S, Singh TR, Chauhan RS. Mining NGS transcriptomes for MiRNAs and dissecting their role in regulating growth, development, and secondary metabolites production in different organs of a medicinal herb, *Picrorhiza Kurroa*. Planta. 2015;241(5):1255–68.
32. Wang YL, Wang YQ, Song ZQ, Zhang HY. Repression of MYBL2 by both microRNA858a and HY5 leads to the activation of anthocyanin biosynthetic pathway in *Arabidopsis*. Mol Plant. 2016;9(10):1395–405.
33. Chen YB, Liao BB, Lin XH, Luo QS, Huang XY, Wang XJ, Shan QL, Wang YQ. Integrative analysis of MiRNAs and their targets involved in ray floret growth in *Gerbera hybrida*. Int J Mol Sci. 2022;23(13):7296.
34. Wei G, Xu MM, Shi XW, Wang Y, Shi YQ, Wang JW, Feng LG. Integrative analysis of MiRNA profile and degradome reveals post-transcription regulation involved in fragrance formation of *Rosa rugosa*. Int J Biol Macromol. 2024;279:135266.
35. Shi Y, Xia H, Cheng XT, Zhang LB. Genome-wide MiRNA analysis and integrated network for flavonoid biosynthesis in *Osmanthus Fragrans*. BMC Genomics. 2021;22(1):141.
36. Wang JW, Czech B, Weigel D. miR156-regulated SPL transcription factors define an endogenous flowering pathway in *Arabidopsis Thaliana*. Cell. 2009;138(4):738–49.
37. Jiao YQ, Wang YH, Xue DW, Wang J, Yan MX, Liu G, Dong GJ, Zeng DL, Lu ZF, Zhu XD, Qian Q, Li JY. Regulation of *OsSPL14* by OsmiR156 defines ideal plant architecture in rice. Nat Genet. 2010;42(6):541–4.
38. Zhang, J., Yang, Y., Wang, Z.P., Li, X.Y., Sun, H.M., 2021. Evidence of the regulatory roles of candidate miRNAs during somatic embryogenesis in Lilium davidii var. unicolor. J Plant Growth Regul, 40:197–214.
39. Parreira JR, Cappuccio M, Balestrazzi A, Fevereiro P, Araújo SS. MicroRNAs expression dynamics reveal post-transcriptional mechanisms regulating seed development in *Phaseolus vulgaris* L. Hortic Res. 2021;8(1):18.
40. Roy S, Tripathi AM, Yadav A, Mishra P, Nautiyal CS. Identification and expression analyses of MiRNAs from two contrasting flower color cultivars of Canna by deep sequencing. PLoS ONE. 2016;11(1):e0147499.
41. Yang JH, Liu XY, Xu BC, Zhao N, Yang XD, Zhang MF. Identification of MiRNAs and their targets using high-throughput sequencing and degradome analysis in cytoplasmic male-sterile and its maintainer fertile lines of *Brassica juncea*. BMC Genomics. 2013;14:1–16.
42. Chen X, Zeng Y, Wang J, Chen X, Xiaoping X. Evolutionary characteristics of miR159 gene family in *Dimocarpus Longan* Lour., and their Spatial and Temporal expression. Chin J Appl Environ Biol. 2017;23:602–8.
43. Duan WH, Yan JR, Li L, Song HM, Meng LH, Zhang ZK, Xu XB, Wang Q, Li JK. Silencing Sly-miR167a delayed preharvest ripening of tomato fruit. Postharv Biol Technol. 2024;211:112828.
44. Gutierrez L, Bussell JD, Pacurar DI, Schwambach J, Pacurar M, Bellini C. Phenotypic plasticity of adventitious rooting in *Arabidopsis* is controlled by complex regulation of AUXIN RESPONSE FACTOR transcripts and MicroRNA abundance. Plant Cell. 2009;21(10):3119–32.
45. Rong FX, Lv YS, Deng PC, Wu X, Zhang YQ, Yue EK, Shen YX, Muhammad S, Ni FR, Bian HW, Wei XJ, Zhou WJ, Hu PS, Wu L. Switching action modes of miR408-5p mediates auxin signaling in rice. Nat Commun. 2024;15(1):2525.
46. Chen J, Pan A, He SJ, Su P, Yuan XL, Zhu SW, Liu Z. Different MicroRNA families involved in regulating high temperature stress response during cotton (*Gossypium hirsutum* L.) anther development. Int J Mol Sci. 2020;21(4):1280.
47. Zhou R, Yu XQ, Ottosen CO, Zhang TL, Wu Z, Zhao TM. Unique MiRNAs and their targets in tomato leaf responding to combined drought and heat stress. BMC Plant Biol. 2020;20(1):107.
48. Han X, Zhang JH, Han S, Chong SL, Meng GL, Song MY, Wang Y, Zhou SC, Liu CC, Lou LH. The chromosome-scale genome of *Phoebe Bournei* reveals contrasting fates of terpene synthase (TPS)-a and TPS-b subfamilies. Plant Commun. 2022;3(6):100410.
49. Yu H, Sole rM, Clemente S, Mila H, Paiva I, Myburg JA, Bouzayen AA, Grima-Pettenati M, Cassan-Wang J, H. Comprehensive genome-wide analysis of the Aux/IAA gene family in Eucalyptus: evidence for the role of EgrIAA4 in wood formation. Plant Cell Physiol. 2015;56(4):700–14.

Publisher's note